IEEE Access
Multidisciplinary | Rapid Review | Open Access Journal

IEEE Power & Energy Society Section

Received 9 May 2024, accepted 27 July 2024, date of publication 7 August 2024, date of current version 22 August 2024.

Digital Object Identifier 10.1109/ACCESS.2024.3439724

APPLIED RESEARCH

A Wildfire Progression Simulation and Risk-Rating Methodology for Power Grid Infrastructure

BEHROUZ SOHRABI[1], (Member, IEEE), ALI ARABNYA[1,2], (Senior Member, IEEE), MATTHEW P. THOMPSON[3], AND AMIN KHODAEI[1], (Senior Member, IEEE)

[1]Department of Electrical and Computer Engineering, University of Denver, Denver, CO 80208, USA
[2]Quanta Technology, Raleigh, NC 27607, USA
[3]Pyrologix, Missoula, MT 59802, USA

Corresponding author: Amin Khodaei (amin.khodaei@du.edu)

This work was supported in part by the Rocky Mountain Research Station, USDA, under Grant 22-CS-11221636-121.

ABSTRACT As the frequency and intensity of power line-induced wildfires increase due to climate-, human-, and infrastructure-related risk drivers, maintaining power system resilience and reducing environmental impacts become increasingly crucial. This paper presents a comprehensive methodology to assess the susceptibility, vulnerability, and risk of power line-induced wildfires for lines and nodes in an electric grid. The methodology integrates a well-established wildfire spread simulator into power flow analysis through a set of analytical steps. The proposed approach is applied to a case study using the IEEE 30-bus test system mapped on a region in the Yosemite-Ritter section of the Sierra Nevada in California. The main findings include the identification of high-risk lines and high-impact nodes and quantification of their vulnerability. These insights can inform the implementation of microgrids, virtual power plants, and distributed energy resources (DERs) to increase grid resilience and guide risk mitigation efforts such as line undergrounding, vegetation management, and maintenance procedures. The proposed methodology intends to provide an effective tool for power system planners and operators to assess the risk exposure of their grid to power line-induced wildfires, enabling them to make informed decisions for allocating capital to their resilience building and risk mitigation strategies.

INDEX TERMS Power systems, resilience, risk assessment, transmission lines, vulnerability analysis, wildfire.

I. INTRODUCTION

The National Oceanic and Atmospheric Administration (NOAA) reports indicate a significant rise in the impact of wildfires over recent decades. From 1994 to 2003, wildfires caused an inflation-adjusted $12.2 billion in damages and 43 deaths. The next decade saw a slight increase to $14.5 billion and 79 deaths. However, from 2014 to 2023, damages escalated dramatically to $106.5 billion with 369 lives lost [1]. This growing threat poses a significant challenge to the civil infrastructure systems, as well as the safety and economic wellbeing of the communities residing in wildfire-prone areas. The keystone of modern society is a resilient power grid that ensures an uninterrupted supply of electricity to citizens and interdependent lifeline systems even during extreme events. Recent disasters in the western U.S. have underscored the need to rethink and transform traditional approaches to wildfire management while predicting and preventing power line-induced wildfires. The 2018 Camp fire in Northern California—which was sparked by PG&E's electrical infrastructure—took 85 lives, burned a total of 153,336 acres, destroyed more than 18,800 homes and structures, and made PG&E face a multibillion-dollar lawsuit as a result [2], [3]. Wildfires ignited by power grids can result in substantial impacts on both the environment and the grid itself and can cause widespread power outages. The Dixie Fire in Northern California in 2021 is a microcosm of recent catastrophic wildfires caused by power lines, which burned over 963,000 acres

The associate editor coordinating the review of this manuscript and approving it for publication was Ha Nguyen.

and destroyed thousands of structures [4]. This devastating fire not only caused extensive damage to the power infrastructure but also led to widespread outages, as utility companies were forced to shut down parts of the grid and implement preemptive measures, such as Public Safety Power Shutoffs (PSPS), to prevent further spread of the fires [5]. Fig. 1 highlights the growing trend of wildfires ignited by power grids over time among other causes of wildfires in the U.S. from 1992 to 2020—emphasizing the increasing importance of mitigating these incidents. Fig. 2 compares the frequency to the average burned area (impact) for different causes of wildfire incidents in the U.S. from 1992 to 2020. As the historical data advocates, the impact of wildfires caused by the grid is significant compared to many other incidents [6]. While power grids are responsible for less than 10% of wildfire ignitions, they are responsible for more than 90% of fatal wildfires in Australia. In California, power lines are responsible for igniting four out of 20 most massive wildfires by acreage burned, and five out of 20 largest wildfires by structures destroyed. The cost of power line-induced wildfires in Northern and Southern California was about 99% of the total cost for all fires [7].

Several studies [8], [9], [10] have identified the main types of faults responsible for major wildfires triggered by power grid failures: a) electric arc without physical contact, where a high-voltage current arcs through the air and ignites nearby vegetation or other combustible materials; b) structural failure of grid components, including rupture of cables, fracturing of poles and supports, failures at splice joints or anchor points, and transformer explosions. These incidents lead to sparks or live wires falling, potentially igniting the surrounding area; and c) external interference which occurs when objects such as trees, branches, or animals fall onto or contact power lines. This can cause short circuits or physical damage to the power infrastructure, leading to the emission of sparks or molten metal particles that can ignite nearby fuel.

The scale of power line-induced wildfires highlights their significance, as their impact on other parts of the grid expands beyond their initial ignition point, correlating with the extent of exposed infrastructure. Therefore, understanding the susceptibility, vulnerability, and risk of these extreme events on transmission lines and nodes is crucial for power system planners to develop effective strategies for managing the grid resilience. Risk assessment helps identify which transmission lines are more likely to cause significant outages and damage to the environment when ignites a wildfire, allowing planners to optimize their asset management strategy including corrective and preventive maintenance, system upgrades, infrastructure hardening, and vegetation management for critical components. Impact assessment shows how much outage a node will face on average when a line is impacted by wildfires. Susceptibility assessment, on the other hand, identifies nodes and lines that are more susceptible to the impacts of wildfires ignited from other locations, providing insights into the weak points within the grid that require reinforcement. Focusing on these crucial areas can inform the risk management strategy for resilience building measures in the face of wildfires including a) prevention strategy, b) mitigation and proactive response, and c) recovery preparedness [11]. Additionally, the understanding of susceptibility, vulnerability, and risk measures can inform targeted asset management strategies, ensuring that investments are made in the most effective manner to maintain and upgrade grid components.

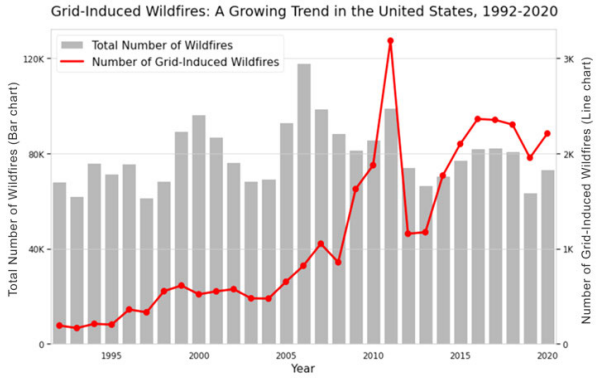

FIGURE 1. Trend of wildfires caused by the grid over time [6].

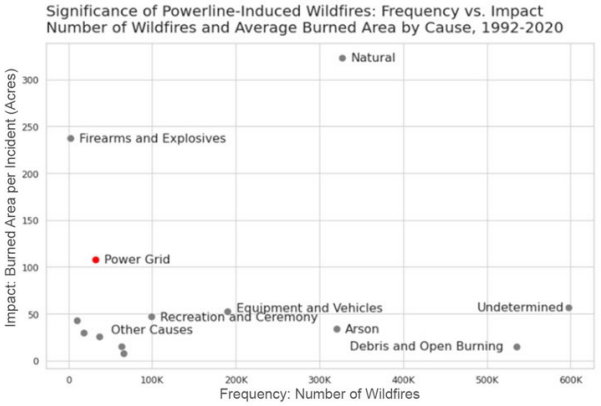

FIGURE 2. Frequency and impact comparison for wildfire causes [6].

II. LITERATURE REVIEW

With the rise in power line-induced wildfires in recent years and their substantial impact on power systems, the need for extensive research into wildfire risk assessment, prevention, detection, mitigation, and resilience enhancement regarding power grids is evident. There has been a significant increase in research at the intersection of power grids and wildfire risk management. This literature review examines the key advancements and methodologies in this area, summarizing their main contributions.

Several studies have addressed power line-induced wildfire prevention and risk mitigation strategies. Studies in [12], [13], [14], [15], and [16] investigate measures adopted by electric utilities for wildfire prevention and response. These measures

encompass monitoring and clearing vegetation near transmission lines, fault detection strategies, equipment maintenance, enhanced inspection and monitoring standards, various grid hardening actions, and the application of PSPS and operational best practices. Authors in [17] present a framework using historical wildfire data to quantify power line risks. This framework employs an optimization model based on the determined risk map to prioritize which overhead lines should convert to underground cables, reducing wildfire risk. Taking a more data-driven approach, [18] combines the latest electrical protection technology, statistical forecasting, meteorological data, and regional risk modeling to promote a proactive wildfire prevention strategy, guiding utilities in improving grid operations. The study in [19] evaluates the use of PSPS as a countermeasure against power line-induced wildfires during adverse weather conditions, providing a methodology for selecting specific grid segments for de-energization to reduce risk. Expanding upon this theme, the study in [20] offers an optimization model based on wildfire risks and efficient post-event restoration in regions vulnerable to wildfires to guide utilities on targeted power shutoffs, updating recommendations based on fresh forecast data. Authors in [21] present a data-driven approach to reduce the computation time needed for power flow analysis, which is crucial for PSPS planning during wildfires. Authors in [22] present an optimization model designed to reduce wildfire risks by enhancing grid operations during PSPS events and determining the best options for placing and investing in infrastructure, including grid-scale batteries, solar PV, and line-hardening measures. From a cost-benefit standpoint, [23] quantifies potential monetary losses due to wildfires and contrasts them with the costs of fire-resilient retrofitting measures. It evaluates the economic implications of retrofitting transmission lines in a practical grid to mitigate wildfire risks.

Transitioning from wildfire prevention and mitigation strategies, other studies have turned their focus to the development of methods for the early detection of power line-induced wildfires. The rising severity of wildfires, as pointed out in [24], is partially linked to faults in electric utility distribution circuits. Building on this observation, the study utilizes waveform analytic techniques and real-time monitoring to introduce a real-time diagnostic technique, designed to detect potential fire ignition mechanisms before they escalate. Reference [25] delves deeper into the understanding of vegetation ignition characteristics and, using real-world data, proposes a Hybrid Step XGBoost (HSXG) model to pinpoint hazardous powerline-vegetation contacts, emphasizing early wildfire detection. Meanwhile, in [26], a shift is seen towards harnessing the power of real-time deep learning algorithms, aiming to accurately classify and locate faults in power distribution grids that may trigger potential fires. Similarly, [27] targets early detection, presenting a methodology geared towards the precise prediction of wildfire ignition risks, with a special focus on high impedance faults.

Another critical avenue of research focuses on grid resilience and adapting operations under the stress of wildfire incidents. The study in [28] explains that the challenges of enhancing resilience against wildfires include real-time responses, situational awareness, preventive measures, proactive corrections, and dynamic restoration strategies. Building on this, [29] presents a proactive generation redispatch strategy to enhance power grid resilience during wildfires, utilizing a Markov decision process (MDP). In [30], the authors present a framework to assess the impact of electric vehicle (EV) evacuations and associated charging demands on grid resilience amid wildfire events, underscoring the growing significance of power system planning and operations during such extreme events. The study in [31] proposes an optimization-based approach for grid expansion planning to balance both wildfire risk and reliable power provision, focusing on the addition of new power lines, modification of existing lines, and the integration of DERs. Other studies, including [32], [33], [13], and [15], have focused on the role of DERs, microgrids, grid-hardening, and grid modernization, to enhance grid resilience and minimize the potential impacts of wildfire on the grid. The study in [34] examines the physical byproducts of wildfires, such as heat, smoke, and ash, and formulates models to assess their impacts on power lines, renewable energy sources, and vital electrical infrastructure that can aid in the management and adaptation of the grid during wildfires. Similarly, [35] investigates how the intense heat from wildfires affects the operational capacity of power lines in their proximity, leading to potential disruptions and degradation of the infrastructure.

Shifting the focus to power line-induced wildfire risk assessment, a pivotal aspect of this study, the literature offers different techniques and methodologies. Using historical data as a foundation, [37] employs wildfire risk maps and powerline locations to assess the risk of powerline-ignited wildfire ignition. Building upon the historical approach, [18] integrates machine learning and past wildfire incidents to formulate a time series forecasting model for estimating the risk of wildfires in relation to power systems. Similarly, [36] leverages machine learning models combined with weather, vegetation, and terrain data to pinpoint wildfire risk probabilities in powerline-adjacent regions. Technical factors play a role in risk prediction as well. For instance, [37] highlights a notable correlation between escalating wind speeds and powerline system failures, which can instigate wildfires. Delving deeper into predictive measures, [19] adopts a surrogate machine learning model to anticipate wildfire ignition risks for individual powerlines under extreme climatic conditions. Broadening the scope, [38] integrates wildfire simulation with forest landscape composition modeling, aiming to assess wildfire threats to a powerline corridor. Finally, [39] merges historical insights with real-time monitoring to devise a comprehensive method for evaluating wildfire dangers within power transmission line corridors.

Despite the vast array of research, there remains a gap for an integrated framework that combines deterministic simulations and analyses, geographical information, and grid topology to assess the risk of power line-induced wildfires towards other components as well as the susceptibility of these components to wildfires. Additionally, there is limited research on the incorporation of wildfire spread simulations to analyze the impact of these incidents on the grid and quantify the resulting damage. This paper bridges these gaps by introducing a novel framework that merges a reliable wildfire spread simulator, FARSITE [40], with power flow analysis and analytical procedures. This approach evaluates the metrics of susceptibility, vulnerability, and risk of lines and nodes in a power grid against power line-induced wildfires. The framework is tested on a case study using the IEEE 30-bus test system [41], a commonly used test system in power system studies, mapped on a region in California. The proposed framework is designed to support the planning, operations, and maintenance of power grids, thereby enhancing grid resilience and improving wildfire risk mitigation strategies in regions highly susceptible to wildfires.

III. MODEL OUTLINE AND PROBLEM FORMULATION

The methodology for developing the framework in this study consists of several steps that integrate a wildfire spread simulator with power flow analysis. The primary goal is to quantify susceptibility, vulnerability, and risk, identify areas prone to wildfires, and determine high-risk components. The proposed steps are as follows:

A. CLOSING THE DATA GAP

The first step in our methodology involves the acquisition of essential data sets, which are crucial for both the run of the FARSITE simulator and the subsequent analysis of its impact on the power grid. These datasets include grid topology, weather conditions, and landscape data for the region under consideration.

The first layer of the dataset consists of grid topology data, which maps the structure of the power grid, detailing the locations and connections of nodes and lines. This specific information is crucial, not only for identifying which lines might be tripped and which nodes could be impacted by the spread of wildfires but also for analyzing how power flows across the grid and how it may be affected by wildfire spread in the post-simulation analysis.

The second layer encompasses weather data, which without loss of generality could be historical, or synthetically generated using statistical parameters for extreme conditions. This feature data is a statistically significant predictor of the ignition and spread of wildfires and includes factors such as temperature, humidity, wind speed, and wind direction of the investigated region which are all integral to accurately simulating wildfire spread and behavior [40], [42]. Specifically, these parameters are essential inputs for the FARSITE wildfire simulator, ensuring it captures the dynamic nature of such incidents comprehensively.

The third layer comprises landscape and fuel data, essential for capturing a realistic representation of wildfire behavior, which includes topographic details of the landscape such as elevation, slope, solar aspect, and barriers, along with landscape fuel properties including fuel model, canopy cover percentage, crown height, crown base height, and crown bulk density. Each parameter plays a unique role in the behavior and progression of wildfires [40]. For instance, elevation and slope directly affect the speed and direction of fire spread, with fires generally moving faster uphill due to the preheating of fuels positioned ahead the flames. The solar aspect determines which part of the landscape is most exposed to sunlight, influencing fuel dryness and, therefore, its combustibility. Properties such as the fuel flammability model and canopy cover percentage influence how easily a fire will ignite and spread through specific types of vegetation. The crown height, base height, and bulk density are crucial for predicting the potential of crown fires, which rapidly propagate through the canopy or treetops and cause spotting. This can allow the fire to jump barriers and ignite new fires away from the main blaze. As a comprehensive simulator, FARSITE requires these detailed inputs to produce accurate simulations that capture the complex behavior of wildfires. Ensuring that this data accurately represents the region is crucial for generating reliable wildfire spread simulations. Fire spread calibration based on historic fires, as an important step of using fire simulation systems, could potentially help improve the results accuracy. Collecting these layers provides a solid foundation for the subsequent steps of the methodology.

B. WILDFIRE SCENARIOS GENERATION

The second step involves generating a diverse set of wildfire ignition scenarios, simulating the conditions under which hypothetical wildfires ignite and propagate. These scenarios should be designed to cover a broad range of possibilities for the system under study to thoroughly analyze the risks and vulnerabilities of its components. As previously highlighted, variations in weather conditions, such as wind speed and direction, temperature, and humidity, can drastically alter wildfire behavior. These variations must be incorporated into the scenarios.

Furthermore, ignition locations must be strategically placed along transmission lines and high-risk grid areas to simulate power line-induced wildfire ignition. These points can be positioned at equal intervals on the lines for systematic coverage. Alternatively, by leveraging risk maps, additional points can be placed in identified hotspots, emphasizing areas with a higher likelihood of fire ignition. Considering the historical patterns of ignition as well as historical fire weather data could play a significant role in improving the accuracy of the obtained results. These important factors will be discussed and investigated in detail in a follow-up work.

This dual approach, which evaluates each potential ignition location under varying weather conditions, forms the foundation of our wildfire scenarios. It contributes

to a comprehensive representation of potential power line-induced wildfire behavior. This extensive suite of scenarios facilitates an in-depth exploration of how wildfires might interact with and impact the power grid, providing valuable insights into system vulnerabilities and resilience.

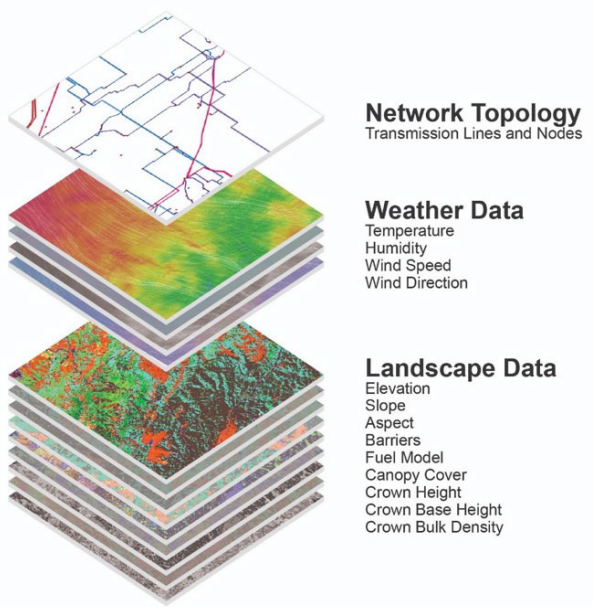

FIGURE 3. The Multi-Layered Data Foundation for the Framework.

C. WILDFIRE SPREAD SIMULATION

In this step, wildfire scenarios and landscape data are fed into the FARSITE simulator to determine the areas affected by wildfire in each scenario. Developed by Mark Finney, FARSITE models the spread of wildfires using a detailed spatiotemporal and deterministic simulation process. The modeling approach of FARSITE utilizes Huygens' principle of wave propagation to simulate the advancement of a fire front. The model incorporates several sub-models of fire behavior, including surface fire, crown fire spread, fire acceleration, fuel moisture, and spotting from torching trees. All these calculations pertain to the perimeter of the fire, primarily advancing the fire edge according to Huygens' principle. FARSITE dynamically divides the simulation into discrete time steps. Within each step, the model calculates the progression and behavior of wildfire which is represented as a continuously expanding polygon defined by a series of vertices.

FARSITE structures its simulation through a series of timesteps, wherein each timestep computes the growth of a fire polygon by aggregating spread from its vertices. This holistic growth is shaped by the fire's Rate of Spread (ROS) at each vertex of the fire edge. Beyond the ROS, FARSITE also provides critical insights into other aspects of fire behavior. These include the Flame Length, which offers an estimate of the flame height and is crucial for understanding the potential heat intensity and fire severity. The model calculates Crown Fire Activity, indicating whether a fire is surface-based or has transitioned into the canopy, a critical factor for predicting fire spread in forested areas. Additionally, FARSITE outputs the Fireline Intensity, which quantifies the energy output along the fire front and is essential for fire suppression strategies. Instead of using a fixed timestep, FARSITE dynamically modifies it based on the distance resolution, which signifies the furthest horizontal spread allowed before new landscape data is required. To preserve the fire's shape integrity, new vertices are inserted between any two points on the simulated wildfire perimeter that become excessively distant. This process maintains a depiction of the fire that is consistent with the model's parameters and responsive to environmental variations, enhancing the simulation's accuracy across diverse terrains. However, like any deterministic simulator, FARSITE can encounter inaccuracies, primarily due to challenges in securing reliable input data with the necessary spatial and temporal resolution [47]. Despite these challenges, FARSITE has proven to be a robust tool, especially when equipped with accurate data. It is recognized by numerous federal land management agencies not only as an essential instrument for predicting fire growth but also as a valuable resource for broader fire management applications [42], [43].

Our choice of FARSITE for our framework is driven by its proven reliability and its capability to model intricate wildfire interactions in diverse terrains. The detailed output from FARSITE simulations depicts the intensity, progression, and extent of each wildfire scenario, identifying areas of the power grid directly impacted by the wildfires. This provides a detailed dataset for subsequent steps in the methodology. Canopy height near powerlines can be used in the simulations to assess potential impact. However, for simplicity, a 2D perspective approach is leveraged in this paper. This topic will be explored in detail in a future work.

D. IMPACT ANALYSIS

Following the wildfire spread simulation, a data-driven impact analysis is conducted to evaluate the repercussions of each scenario on the grid. The output from the FARSITE simulator, which includes detailed wildfire perimeters, fire intensity, and fire arrival time, is integrated with the spatial coordinates of grid components. Through spatial analysis, the lines and nodes exposed to the wildfire in each simulation scenario are identified. These affected components represent potential points of failure or disruption in the grid. The result of this step is a comprehensive mapping of which grid components are likely to be impacted in a given scenario, serving as an input for subsequent steps in the methodology. Fig. 4 illustrates the spatial intersection of the simulated wildfire spread output overlaid by the geographical layout of the grid, showing the components directly affected by the fire. Canopy height near power lines can be used in the simulations to assess potential impact.

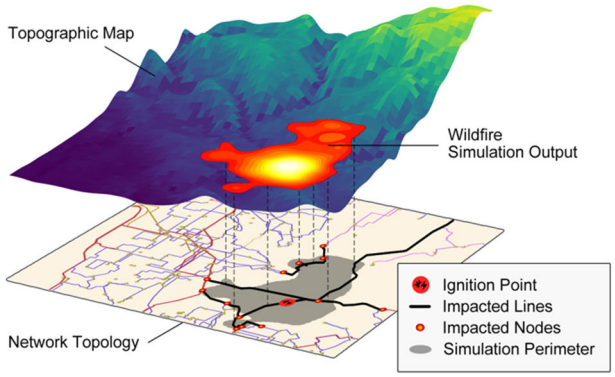

FIGURE 4. Wildfire Simulation Output Mapped with the Grid Topology.

E. GRID MODIFICATION

Once the impacted lines and nodes are identified, the next step involves modifying the grid's component specifications based on the results of the impact analysis for each scenario. This modification is intended to simulate the changes in the operational state of the grid due to the faults caused by wildfires. For instance, a transmission line intersecting with a wildfire may be considered damaged or at risk of failure and thus may be rendered non-operational in the modified grid. Similarly, nodes within the wildfire perimeter might experience reduced capacity or total outage depending on the extent of the fire impact. The extent of fire represents the impact of wildfire on the power grid, resulting in potential power outages. These modifications are then integrated into the power grid model. This approach ensures that the subsequent power flow analysis considers the potential impacts of wildfire in each scenario on grid operation.

To account for potential outages (i.e., load curtailment) in the power flow analysis, virtual high-cost generators are placed at each load node. These generators are considered ''virtual'' because they do not represent actual generators, but rather function as negative loads to simulate a scenario when the load cannot be fully supplied. These generators are designated as ''high cost'' to reflect the undesirable nature of power outages. Under normal operating conditions, the power system is always inclined to utilize lower-cost actual power generators. Resorting to these high-cost virtual generators in the model signifies that the system is under stress and must use more expensive means, here load curtailment, to maintain a stable power flow. Therefore, they act as a useful tool in our simulations to understand the magnitude of power outages at each node under various wildfire scenarios and inform the placement of real power sources, such as microgrids and DERs, to increase resilience.

F. POWER FLOW ANALYSIS

In this phase, an AC optimal power flow (ACOPF) analysis is performed for each scenario on the modified grid. The primary purpose of this analysis is to calculate the steady-state operational conditions of the power grid post-wildfire incident. The ACOPF problem can be stated mathematically as an optimization problem with an objective function and several constraints. The goal is to minimize the total cost of power generation while maintaining the system within its operational limits [44]. The formulation of the ACOPF problem is as follows:

$$\min \sum_{i \in G} C_i \left(P_i^g\right), \tag{1}$$

where $C_i\left(P_i^g\right)$ represents the cost of power generation by generator i, and G is the set of all generators. The variables for optimization are the real power and reactive power outputs from each generator (P_i^g and Q_i^g), and the voltages at each bus (V_n). The main constraints to be satisfied include power balance, generation limits, and power flow constraints.

The power balance constraints (2) and (3) ensure that the total generated power plus the power injected through transmission lines equals the total demand, separately for both real and reactive power, at each node. In mathematical terms:

$$P_n^g + P_n^c - P_n^d + P_n^l = 0 \quad \forall n \in N, \tag{2}$$
$$Q_n^g + Q_n^c - Q_n^d + Q_n^l = 0 \quad \forall n \in N, \tag{3}$$

where P_n^g and Q_n^g are the real and reactive power generated at node n, P_n^c and Q_n^c are the real and reactive power generation from high-cost generators at node n, P_n^d and Q_n^d are the real and reactive power demand at node n, P_n^l and Q_n^l are the real and reactive power flows injected to node n. N is the set of all nodes. Each generator's output should not exceed its maximum capacity nor fall below its minimum as shown in (4) and (5), respectively.

$$P_i^{min} \leq P_i^g \leq P_i^{max} \quad \forall i \in G, \tag{4}$$
$$Q_i^{min} \leq Q_i^g \leq Q_i^{max} \quad \forall i \in G, \tag{5}$$

where $P_i^{min}, P_i^{max}, Q_i^{min}$, and Q_i^{max} represent the minimum and maximum limits for real and reactive power for generator i respectively.

The voltage magnitude at each bus should stay within a specified range to ensure safe and efficient operation (6), where V_n is the voltage at node n, and V_n^{min} and V_n^{max} are respectively the associated minimum and maximum permissible voltage magnitudes.

$$V_n^{min} \leq |V_n| \leq V_n^{max} \quad \forall n \in N, \tag{6}$$

The power flow on each transmission line should not exceed its rated capacity to prevent line overheating and potential failures. The power flow equations for the lines connecting different buses can be represented in terms of real and reactive power flows. Considering the nodal voltages, impedance, and the angle differences between connected nodes, the line flow equations are:

$$P_{nm} = V_n \sum_{k \in N_n} V_k (G_{nk} \cos\theta_{nk} + B_{nk} \sin\theta_{nk}) \ \forall n, m \in N, \tag{7}$$

$$Q_{nm} = V_n \sum_{k \in N_n} V_k (G_{nk} \sin\theta_{nk} - B_{nk} \cos\theta_{nk}) \ \forall n, m \in N, \tag{8}$$

where V_n and V_k are the voltage magnitudes at buses n and k respectively, θ_{nk} denotes the angle differences between the voltages at buses n and k, G_{nk} and B_{nk} are the conductance and susceptance of the line connecting buses n and k respectively, and N_n represents the set of buses connected to bus n. The line flow should also adhere to its limits:

$$P_{nm}^{min} \leq P_{nm} \leq P_{nm}^{max} \quad \forall n, m \in N, \tag{9}$$

where P_{nm}^{min} and P_{nm}^{max} are the minimum and maximum real power flows for the line connecting nodes n and m, respectively.

In this process, the use of virtual high-cost generators at each node guarantees the feasibility of power flow, even under the stress of component outages. Thus, the power flow analysis produces a feasible solution and provides insights into how the grid should optimally adapt and respond to the impacts of wildfire incidents. The outcome of the ACOPF analysis offers vital information on power flows, voltages, generator outputs, and outages for each scenario. This data reveals the power grid's performance under different wildfire conditions, helping in quantifying measures of susceptibility, vulnerability, and risk.

G. DATA ANALYSIS

Once the power flow analysis is completed for all scenarios, the next step is to analyze the obtained data to derive the metrics, each represented as a dimensionless ratio.

1) SUSCEPTIBILITY

Susceptibility is defined as the potential of system components, including lines and substations, to be affected by and susceptible to ignition from the system's powerline-induced wildfires. The susceptibility of a particular node (U_n^{node}) or line (U_j^{line}) can be quantified by counting the number of times it is affected across all scenarios.

$$U_n^{node} = \frac{1}{|Z|} \sum_{s \in Z} A_{ns}, \tag{10}$$

$$U_j^{line} = \frac{1}{|\bar{Z}|} \sum_{s \in Z} A_{js}, \tag{11}$$

where A_{ns} and A_{js} are binary values representing whether node n and line j are affected in scenario (s) out of all scenarios (Z). A line is considered affected when it falls within the wildfire simulation's perimeter, and a node is considered affected when a line connected to it or the node itself is caught in the perimeter.

2) RISK

Risk is defined as the expected operational impact on the overall grid's reliability and service continuity due to the failure of a particular component (in this case, a transmission line) which ignites a wildfire and leads to subsequent failures within the grid. The risk associated with each line (R_j) is calculated by taking the average of power outages ignited by line j. In this equation P_{jsn}^{o} represents the amount of power outage caused by line j in scenario s at node n.

$$R_j = \frac{1}{\left|Z_j'\right| |N|} \sum_{s \in Z_j'} \sum_{n \in N} \frac{P_{jsn}^{o}}{P_n^d}, \tag{12}$$

3) VULNERABILITY

The vulnerability associated with each node (I_n) is the degree to which the node is susceptible to power outages, measured as the average power outage at each node across all simulated wildfire scenarios. It reflects the potential service disruption due to wildfires ignited by power lines within the grid. In essence, vulnerability offers a holistic view of how a node can be impacted by power outages across a set of wildfire scenarios.

$$I_n = \frac{1}{|Z|\,|L|} \sum_{s \in Z} \sum_{j \in L} \frac{P_{jsn}^{o}}{P_n^d}. \tag{13}$$

IV. CASE STUDY

The proposed methodology was implemented in a case study utilizing the IEEE 30-bus test system, specifically mapped onto a region in the Yosemite-Ritter section of the Sierra Nevada in California. The study area, situated between latitudes 37.6° and 38.1° and longitudes −120.7° and −120°, spans approximately 820,000 acres (331,840 hectares). This region encompasses a diverse range of barriers and terrain types, lakes, forests, and rural areas. This selection was deliberate, as it allows for a comprehensive evaluation of the methodology's effectiveness in assessing the potential impacts of power line-induced wildfires in regions possessing susceptible landscape characteristics. By including different barrier types and terrain features, the case study provides insights into the resilience of the grid in the face of wildfires, considering the challenges posed by different geographical conditions.

Landscape and fuel data were extracted with a resolution of 60 meters from LANDFIRE [45], a national initiative committed to providing comprehensive geospatial data. LANDFIRE's scope covers vegetation, wildland fuel, and fire regimes across the entirety of the United States, making it a valuable resource for this analysis. In constructing wildfire scenarios, we employed two types of weather datasets to ensure a comprehensive analysis. The scenarios are designed to cover a broad range of weather conditions, from baseline weather patterns to more extreme situations, and include placement of ignition points on each transmission line to simulate potential wildfire initiation points due to power line faults. The detailed breakdown of the scenarios is as follows:

A. IGNITION POINTS AND FIRE IGNITION AREAS

A total of 34 lines, comprising 702 kilometers, were analyzed. Assuming a 1 km distance between fire ignition points, this resulted in a total of 686 distinct ignition points. To further define the ignition areas, a 30-meter buffer zone around the ignition points along powerlines was established.

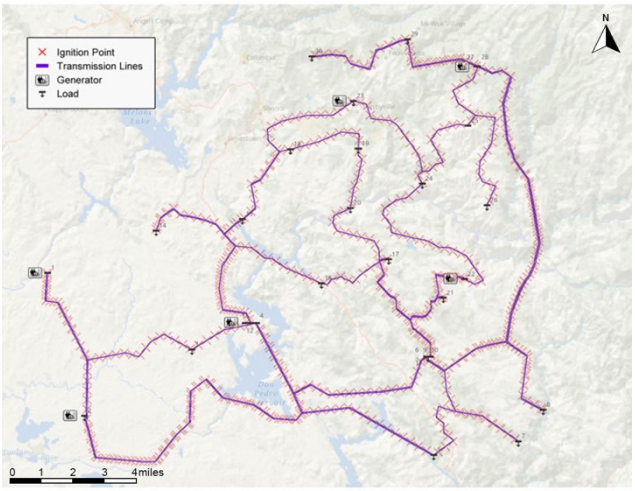

FIGURE 5. Geographic mapping of the IEEE 30-bus test system in the selected region.

B. HISTORICAL WEATHER CONDITIONS

The first set includes two historical weather datasets corresponding to distinct seasonal conditions. Condition 1 represents the fall period, and Condition 2 represents the summer period. These conditions are based on historical weather data borrowed from National Renewable Energy Lab resources [46], providing a realistic baseline for our simulations.

C. EXTREME WEATHER CONDITIONS

The second set comprises four synthetically generated datasets, each emulating severe extreme weather conditions but with distinct dominant wind directions. Specifically, Scenarios 3, 4, 5, and 6 correspond to extreme conditions with dominant wind directions to the North, East, South, and West, respectively. The scenarios were based on a common set of weather parameters indicative of high wildfire risk, including daytime temperatures averaging 35°C fluctuating by a standard deviation of 2°C, and nighttime temperatures averaging 20°C with a standard deviation of 3°C. Wind speeds were considered to have an average of 40 km/h with a 10 km/h standard deviation, and the wind direction was aligned with the dominant direction with a standard deviation of 10 degrees. The relative humidity was set at a low average of 10% with a 5% standard deviation, reflecting the dry conditions conducive to wildfires. Additionally, the scenarios accounted for dead fuel moisture content with an average of 5% and a standard deviation of 2%, highlighting the critical role of fuel conditions in wildfire spread and intensity. Additionally, these conditions were assumed to occur under clear sky days with no cloud cover and no precipitation, further exacerbating the wildfire risk.

This approach led to the generation of a set of 4,116 unique scenarios, encompassing the combination of 686 ignition points under 6 different weather conditions. The extensive suite of scenarios ensures that our analysis captures a wide range of potential wildfire risks to the power grid infrastructure. The landscape data used in this study can be found in [40].

The FARSITE simulations were configured with a spatial resolution of 60 meters, matching the obtained landscape data resolution, and a time step of 30 minutes, balancing detail with computational efficiency. The simulations ran over a burn period of 10 hours, spanning a total duration of 3 days. The crown fire modeling employed the Reinhardt method, and the ember spotting probability was set at 20%.

V. NUMERICAL RESULTS

Following the steps detailed in the methodology section, the discussed metrics for the IEEE 30-bus test system are evaluated. In Tables 1-4, conditions 1 and 2 represent historical weather conditions during fall and summer periods, respectively. Scenarios 3, 4, 5, and 6 correspond to extreme conditions with dominant wind directions to the North, East, South, and West, respectively. MVA (Mega Volt Amperes) is the SI unit for apparent power, representing the product of the root mean square (RMS) voltage and current. MW (Megawatts) is the SI unit for real power that measures the actual energy conversion rate. The values presented in the following tables are the result of calculating the metrics using the outcomes of all 4,116 scenarios.

TABLE 1. Assessed values for susceptibility of lines.

Line	From Node	To Node	Rate (MVA)	Susceptibility of Lines under Various Weather Conditions						
				1	2	3	4	5	6	Mean
1	1	2	130	0.013	0.013	0.024	0.024	0.015	0.027	0.019
2	1	3	130	0.008	0.012	0.017	0.018	0.020	0.020	0.016
3	2	4	65	**0.056**	**0.072**	**0.086**	**0.080**	**0.070**	**0.066**	**0.072**
4	3	4	130	0.016	0.018	0.013	0.015	0.009	0.009	0.013
5	2	5	130	**0.069**	**0.066**	**0.068**	**0.069**	**0.086**	**0.063**	**0.070**
6	2	6	65	**0.081**	**0.090**	**0.109**	**0.100**	**0.101**	**0.101**	**0.097**
7	4	6	90	**0.057**	**0.057**	**0.045**	**0.053**	**0.047**	0.033	**0.049**
8	5	7	70	0.018	0.018	0.012	0.012	0.012	0.015	0.014
9	6	7	130	0.022	0.024	0.028	0.034	0.021	0.027	0.026
10	6	8	32	0.021	0.015	0.017	0.012	0.018	0.009	0.015
17	12	14	32	0.027	0.030	**0.042**	0.036	0.038	**0.053**	0.038
18	12	15	32	0.034	0.036	**0.042**	0.024	0.036	**0.042**	0.036
19	12	16	32	0.039	0.029	0.041	0.032	0.038	**0.042**	0.037
20	14	15	16	0.024	0.013	0.019	0.015	0.013	0.021	0.018
21	16	17	16	0.015	0.028	0.025	0.018	0.018	0.016	0.020
22	15	18	16	0.022	0.019	0.016	0.030	0.019	0.009	0.019
23	18	19	16	0.001	0.001	0.001	0.001	0.004	0.001	0.001
24	19	20	32	0.001	0.003	0.003	0.001	0.004	0.006	0.003
25	10	20	32	0.026	0.041	0.041	**0.042**	0.029	**0.042**	0.037
26	10	17	32	0.027	0.030	0.040	**0.046**	0.040	**0.045**	0.038
27	10	21	32	0.039	0.040	**0.053**	**0.043**	0.037	0.036	0.041
28	10	22	32	**0.057**	**0.057**	**0.052**	**0.055**	0.039	**0.054**	**0.052**
29	21	22	32	0.013	0.012	0.015	0.010	0.019	0.013	0.014
30	15	23	16	0.014	0.015	0.015	0.014	0.014	0.012	0.014
31	22	24	16	0.006	0.003	0.011	0.008	0.008	0.005	0.007
32	23	24	16	0.004	0.001	0.001	0.001	0.006	0.007	0.004
33	24	25	16	0.001	0.004	0.001	0.001	0.003	0.003	0.002
34	25	26	16	0.025	0.010	0.012	0.013	0.012	0.013	0.014
35	25	27	16	0.013	0.016	0.013	0.007	0.012	0.013	0.013
37	27	29	16	0.025	0.028	0.041	0.031	0.024	0.034	0.031
38	27	30	16	0.035	0.041	**0.047**	0.041	**0.044**	**0.044**	**0.042**
39	29	30	16	**0.045**	**0.046**	**0.049**	**0.045**	**0.045**	**0.048**	**0.046**
40	8	28	32	0.014	0.025	0.025	0.028	0.017	0.025	0.022
41	6	28	32	**0.084**	**0.083**	**0.076**	**0.081**	**0.089**	**0.083**	**0.083**

The quantified susceptibility for each line in various weather conditions.

Based on the lines' susceptibility values, lines 3, 5, 6, 7, 28, 30, and 41 stand out, consistently demonstrating the highest susceptibility across all weather conditions, with values exceeding the upper quantile. Notably, line 38 in conditions 3, 5, and 6 also surpasses the upper quantile. Similarly, line 27 in conditions 3 and 4, lines 26 and 25 in conditions 4 and 6, and line 17 in conditions 3 and 6, display a heightened susceptibility. These lines bear higher susceptibility to wildfire effects due to their geographical location and proximity to other lines with heightened fire spread probabilities.

TABLE 2. Assessed values for risk.

Line	From Node	To Node	Rate (MVA)	Risk of Lines under Different Weather Conditions						
				1	2	3	4	5	6	Mean
1	1	2	130	0	0	0	0	0	0	0
2	1	3	130	0.001	0.002	0	0.001	0.001	0.001	0.001
3	2	4	65	0	0.001	0	0.001	0.002	0.001	0.001
4	3	4	130	0	0	0	0	0	0.005	0.001
5	2	5	130	0	0	0.005	0	0	0	0.001
6	2	6	65	0.002	0	0.002	0	0.004	0.001	0.002
7	4	6	90	0	0.005	0.005	0.005	0	0	0.002
8	5	7	70	**0.057**	**0.064**	**0.057**	**0.085**	**0.049**	**0.078**	**0.065**
9	6	7	130	**0.064**	**0.056**	**0.056**	**0.040**	**0.056**	**0.080**	**0.059**
10	6	8	32	**0.038**	**0.068**	**0.060**	**0.053**	**0.068**	**0.105**	**0.065**
17	12	14	32	0.020	0.013	0.016	0.014	0.013	0.016	0.015
18	12	15	32	0.002	0	0.002	0	0	0	0.001
19	12	16	32	0.008	0.016	0.011	0.008	0.009	0.007	0.010
20	14	15	16	0.020	0.010	0.010	0.020	**0.023**	0.015	0.016
21	16	17	16	0	0.007	0.005	0.011	0	0	0.004
22	15	18	16	0	0	0	0	0	0	0
23	18	19	16	0.006	0	0	0.004	0	0	0.002
24	19	20	32	0	0.002	0	0	0.003	0	0.001
25	10	20	32	0	0.003	0.005	0.006	0.006	0.005	0.004
26	10	17	32	0	0	0.003	0	0	0	0.001
27	10	21	32	0	0	0.017	0.017	0.008	0.008	0.008
28	10	22	32	**0.031**	**0.031**	**0.070**	**0.046**	**0.061**	**0.070**	**0.052**
29	21	22	32	0	0	0	0	0	0	0
30	15	23	16	0.001	0.001	0	0	0.002	0	0.001
31	22	24	16	0	0	0	0	0	0	0
32	23	24	16	0.003	0.005	0	0	0	0	0.001
33	24	25	16	0.002	0.005	0.010	0.005	0	0.002	0.004
34	25	26	16	0.018	0.018	0.018	0.018	0.018	0.018	0.018
35	25	27	16	0.004	0	0	0.002	0.002	0.004	0.002
37	27	29	16	**0.067**	**0.066**	**0.069**	**0.072**	**0.072**	**0.069**	**0.069**
38	27	30	16	**0.054**	**0.057**	**0.056**	**0.054**	**0.054**	**0.059**	**0.056**
39	29	30	16	**0.047**	**0.056**	**0.056**	**0.057**	**0.057**	**0.056**	**0.055**
40	8	28	32	**0.023**	0.014	**0.024**	0.007	0.001	0.009	0.013
41	6	28	32	0.003	0	0.001	0.001	0.001	0	0.001

The quantified risk for each line in various weather conditions.

Lines 37, 8, and 10 are of the highest risk, each causing an average of 6% of the system's load being curtailed. Following these, lines 9, 28, 38, and 39 also pose a significant risk, with an average value of around 5%. Line 17 in condition 1, line 20 in conditions 1, 4, 5, and line 40 in conditions 1 and 3, are relatively high-risk lines. Line 34 maintains a consistent mid-risk value across all weather conditions. These high-risk lines indicate potential hotspots from which wildfire initiation could result in severe cascading impacts on other lines and nodes due to their strategic location and surrounding available fuel conditions.

Nodes 10, 13, 14, and 15 exhibit a high susceptibility of 0.48, implying they are directly impacted in nearly half of the total 4,116 scenarios conducted. Nodes 2, 3, 8, and 16 also demonstrate significant susceptibility, with a value of 0.29. The high susceptibility of these nodes stems from their interconnections and dependencies on multiple lines, which increase their susceptibility to the impacts of wildfires.

TABLE 3. Assessed values for susceptibility of nodes.

Node	Demand (MW)	Susceptibility of Nodes under Various Weather Conditions						
		1	2	3	4	5	6	Mean
1	0	0.064	0.064	0.074	0.071	0.067	0.074	0.069
2	21.7	0.281	**0.286**	**0.294**	0.284	**0.294**	**0.305**	**0.291**
3	0	**0.293**	**0.299**	**0.296**	**0.306**	**0.299**	0.284	**0.296**
4	0	0.112	0.115	0.114	0.115	0.098	0.109	0.111
5	3.2	0.067	0.067	0.069	0.067	0.071	0.071	0.069
6	0	0.238	0.259	0.262	0.255	0.246	0.245	0.251
7	3	0.069	0.071	0.076	0.077	0.071	0.069	0.072
8	7.6	**0.293**	**0.299**	**0.296**	**0.306**	**0.299**	0.284	**0.296**
9	0	0.172	0.168	0.169	0.168	0.185	0.166	0.171
10	0	**0.483**	**0.477**	**0.469**	**0.494**	**0.483**	**0.483**	**0.481**
11	22.8	0.061	0.063	0.063	0.066	0.057	0.057	0.061
12	30	0.114	0.115	0.115	0.121	0.117	0.105	0.114
13	0	**0.483**	**0.477**	**0.469**	**0.494**	**0.483**	**0.483**	**0.481**
14	5.8	**0.483**	**0.477**	**0.469**	**0.494**	**0.483**	**0.483**	**0.481**
15	0	**0.483**	**0.477**	**0.469**	**0.494**	**0.483**	**0.483**	**0.481**
16	11.2	**0.293**	**0.299**	**0.296**	**0.306**	**0.299**	0.284	**0.296**
17	6.2	0.069	0.076	0.089	0.076	0.076	0.099	0.081
18	8.2	0.134	0.131	0.136	0.128	0.130	0.134	0.132
19	3.5	0.083	0.071	0.089	0.079	0.083	0.089	0.082
20	9	0.076	0.089	0.093	0.090	0.089	0.092	0.088
21	3.2	0.051	0.048	0.047	0.055	0.048	0.038	0.048
22	9.5	0.025	0.026	0.028	0.023	0.032	0.029	0.027
23	2.2	0.070	0.082	0.085	0.085	0.069	0.087	0.079
24	17.5	0.070	0.070	0.082	0.073	0.066	0.064	0.071
25	8.7	0.071	0.070	0.076	0.071	0.076	0.074	0.073
26	0	0.077	0.069	0.069	0.064	0.069	0.070	0.069
27	3.5	0.047	0.032	0.034	0.035	0.034	0.035	0.036
28	0	0.238	0.259	0.262	0.255	0.246	0.245	0.251
29	2.4	0.069	0.071	0.086	0.070	0.064	0.077	0.073
30	10.6	0.071	0.074	0.079	0.073	0.076	0.076	0.075

The susceptibility metrics for nodes under the given scenarios

Node 30 registers the highest average vulnerability (0.064 for all weather conditions), followed by nodes 27 and 29 (0.036 and 0.038 on average, respectively). These nodes represent the most vulnerable nodes in the system and are strong candidates for reinforcement strategies, such as integration with microgrids.

Figs. 6 and 7 offer a geographical representation of the metrics' mean values across various weather conditions. By integrating the data from the tables into a visual format, the spatial representation highlights areas most susceptible to wildfires and identifies critical infrastructure that need retrofitting and reinforcement. This holistic view provides stakeholders with a clear context, enabling them to grasp the broader implications. In turn, they can strategically allocate resources, implement mitigation measures, and devise preventive actions. Aligning strategies with zones of heightened susceptibility, vulnerability, and risk ensures a reduction in the potential for power line-induced wildfires and paves the way for a more resilient power infrastructure.

Through this analysis, components with consistently high susceptibility across different weather scenarios are identified. Especially during the summer period, represented by condition 2, the grid is at an increased risk due to the

TABLE 4. Assessed values for vulnerability of nodes.

Node	Demand (MW)	Vulnerability under Different Weather Conditions						
		1	2	3	4	5	6	Mean
1	0	0	0	0	0	0	0	0
2	21.7	0	0.001	0.005	0.001	0.001	0.001	0.001
3	0	0	0	0	0	0	0	0
4	0	0	0	0	0	0	0	0
5	3.2	0.003	0.002	0.001	0.001	0.000	0.001	0.001
6	0	0	0	0	0	0	0	0
7	3	0.002	0.004	0.001	0.002	0.003	0.007	0.003
8	7.6	0	0.001	0.001	0.001	0.001	0.001	0
9	0	0	0	0	0	0	0	0
10	0	0	0	0	0	0	0	0
11	22.8	**0.025**	**0.025**	**0.024**	**0.027**	**0.022**	**0.031**	**0.026**
12	30	**0.016**	**0.019**	**0.021**	**0.014**	**0.013**	**0.024**	**0.018**
13	0	0	0	0	0	0	0	0
14	5.8	0	0.001	0.001	0.001	0.001	0.001	0.001
15	0	0	0	0	0	0	0	0
16	11.2	0	0.001	0.001	0.001	0	0.001	0.001
17	6.2	**0.034**	**0.019**	**0.024**	**0.027**	**0.027**	**0.026**	**0.026**
18	8.2	0	0.001	0.001	0.001	0.001	0	0.001
19	3.5	**0.013**	**0.028**	**0.020**	**0.014**	**0.015**	**0.013**	**0.017**
20	9	0	0.003	0.007	0.008	0.003	0.004	0.004
21	3.2	0.002	0.001	0.001	0.004	0.005	0.001	0.002
22	9.5	0.001	0.001	0.001	0.001	0.001	0.001	0.001
23	2.2	0	0.005	0.002	0.001	0.008	0.004	0.003
24	17.5	0.007	0.007	**0.012**	0.007	**0.016**	0.011	0.010
25	8.7	0	0.001	0.001	0.001	0.001	0.001	0.001
26	0	0	0	0	0	0	0	0
27	3.5	**0.047**	**0.032**	**0.034**	**0.036**	**0.034**	**0.036**	**0.036**
28	0	0	0	0	0	0	0	0
29	2.4	**0.035**	**0.037**	**0.039**	**0.040**	**0.038**	**0.039**	**0.038**
30	10.6	**0.058**	**0.063**	**0.068**	**0.063**	**0.063**	**0.066**	**0.064**

The vulnerability metric in Table IV illustrates the nodes that experience the most significant outages due to wildfires.

season's pronounced wildfire hazard. The combination of elevated temperatures and decreased humidity creates drier landscapes, making them more susceptible to both ignition from potential grid-related sparks and the rapid spread of any subsequent wildfires. This seasonal factor amplifies the inherent susceptibility of certain lines and nodes. Moreover, prevailing winds in conditions 3 and 6, directed towards the north and west respectively, intensify the impact on specific components. These effects arise from design considerations, as well as interactions with regional topographical and vegetational factors. On the other hand, while condition 5, associated with wind directed to the south, may have a milder direct impact on most components, lines 6 and 5 display the highest susceptibility compared to other wind conditions. Thus, this condition should not be overlooked.

Even minimal disruptions in such scenarios can result in cascading effects within a tightly interconnected grid. In general, lines 3, 5, 6, 7, 28, 30, 41, and nodes 10, 13, 14, and 15 emerge as the most susceptible to wildfires, attributed to their strategic positions and interconnections within the grid in all weather conditions. The failure of these components could dramatically propagate the wildfire impact across the grid, leading to considerable load shedding. As a direct implication, these high-risk components should be targeted for risk mitigation strategies to reduce the overall system vulnerability. Conversely, nodes such as 30, 27, 29, 11, 17, 12, and 19, which register high outage rates during wildfires, should be prioritized for reinforcement measures. Improving the resilience of these nodes could significantly enhance the system's capacity to withstand and recover from wildfire damages.

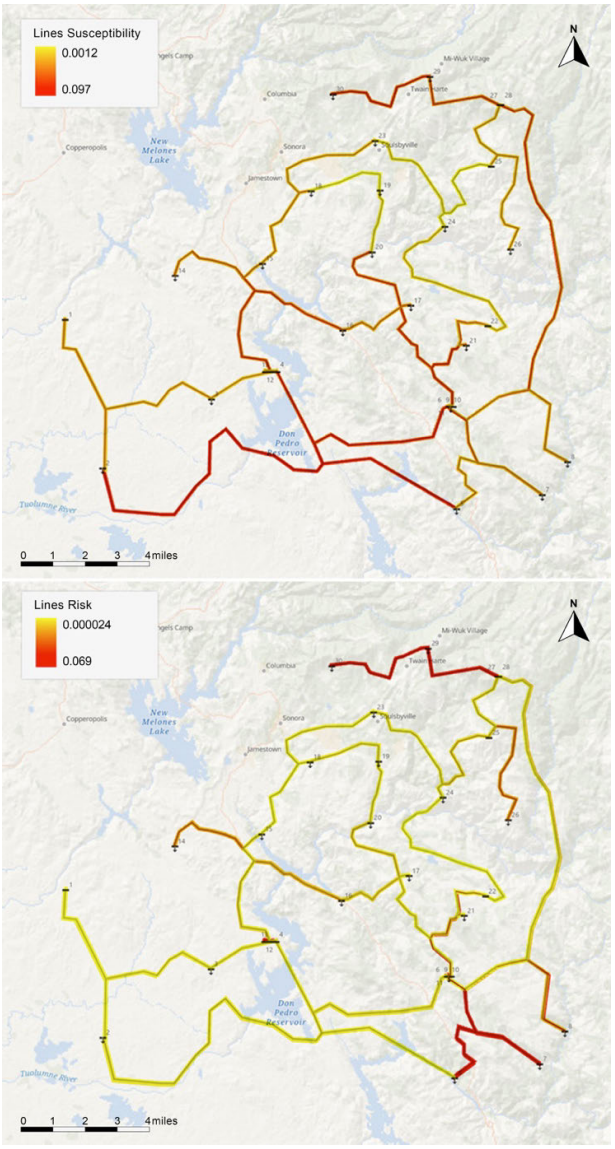

FIGURE 6. Visualization of Average Susceptibility and Risk of Lines.

This analysis offers a roadmap for power system planners and operators, anchoring the design of apt resilience and mitigation methodologies. Taking cues from the derived insights, strategies might encompass the deployment of microgrids and virtual power plants. Additionally, vegetation management, line undergrounding, and proactive asset upgrades and maintenance emerge as other viable countermeasures. The case study demonstrates the proposed methodology's effectiveness in assessing the power grid's components susceptibility, vulnerability, and risk to wildfires. By identifying susceptible, vulnerable, and high-risk lines and nodes, the study

enables informed decision-making on where to concentrate investments for resilience and risk mitigation strategies.

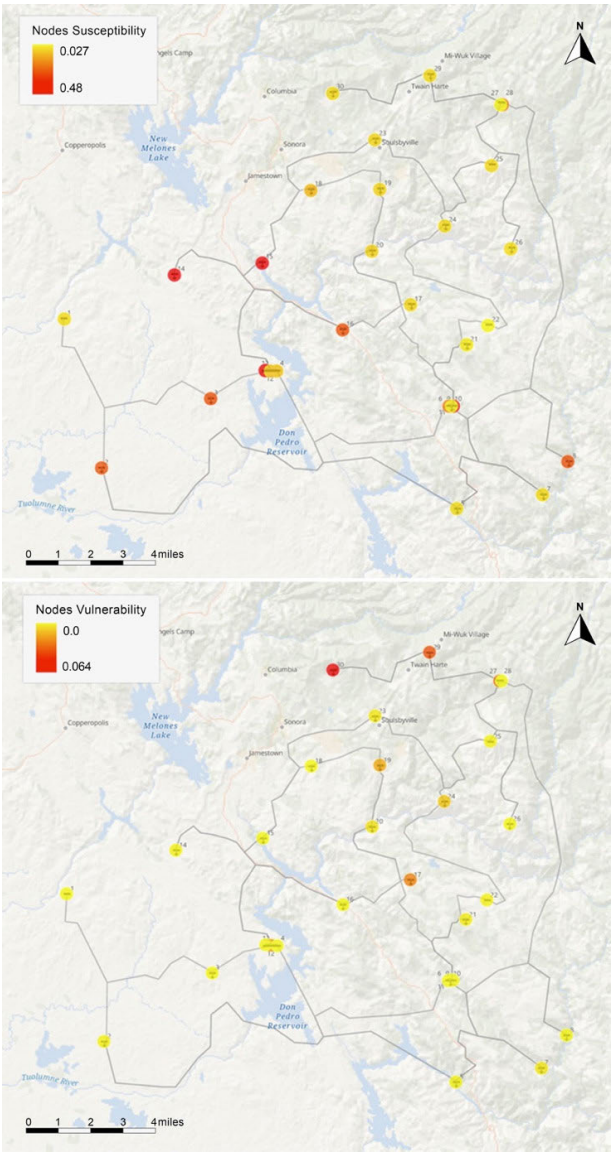

FIGURE 7. Visualization of Average Vulnerabilities and Susceptibility of Nodes.

Our reference to ''strategic locations'' and ''surrounding available conditions'' is derived from our observation of the derived metrics across the grid and the landscape. Specifically, the ''strategic locations'' refer to power grid components—such as transmission lines and nodes—that, due to their geographical positioning and connectivity within the grid, have a higher susceptibility to wildfire risks. These components are identified as having higher susceptibility and risk values in our analysis, indicating their critical role in the grid's overall vulnerability to wildfires. The ''surrounding available conditions'' encompass the combination of topographical and vegetational characteristics of the areas surrounding these components. For instance, lines and nodes identified with high susceptibility and risk values are often located in regions characterized by dense vegetation or in topographical corridors that can channel and accelerate wind-driven fires.

VI. CONCLUSION

We proposed a wildfire risk rating framework that combines a wildfire spread simulator, power flow analysis, landscape data, and grid topology. This framework identifies the risk from power lines and the potential vulnerability of interconnected components due to power line-induced wildfires. It analyzes the grid's susceptibility to wildfires, determines the potential impact on the grid due to the failure of individual transmission lines, and estimates power outages at each node for a pre-defined set of wildfire scenarios. The IEEE 30-bus test system was utilized for a case study to demonstrate the capabilities of the proposed model. Findings suggest that this framework can assist power system planners and operators in making risk-informed decisions for their capital programs and investments in resilience and risk mitigation efforts.

Existing results are based on quantitative studies considering network data and fire spread. Our analysis does not directly use spread probability data; instead, it infers the relative spread probabilities based on the extent of impact on power lines. That is, a power line experiencing greater impact suggests a higher wildfire spread probability in its area.

Furthermore, it is crucial to acknowledge the inherent limitations and potential sources of error that must be considered. These include inaccuracies in user inputs, inherent limitations of the models themselves, and the quality of the data used, especially concerning landscape and weather conditions. Notably, the use of wildfire spread simulators like FARSITE introduces specific challenges, primarily stemming from the complexity of accurately simulating wildfire behavior and the difficulties in securing reliable input data with the necessary spatial and temporal resolution, which can lead to inaccuracies in any deterministic simulator [42], [43], [47].

Future enhancements of this framework will focus on refining the accuracy of these variables, incorporating more detailed historical fire regime data to strategically concentrate ignition points around areas identified as high-risk based on past wildfire occurrences, and enhancing modeling techniques in the impact analysis step utilizing canopy cover condition and power line height. Also, in our work, the metrics for each transmission line are determined across the entire length of the line. Adopting a more granular approach represents a promising direction for future research. These efforts aim to reduce potential errors and further enhance the framework's results reliability.

REFERENCES

[1] NOAA Nat. Centers for Environ. Inf. (NCEI). (2024). *U.S. Billion-Dollar Weather and Climate Disasters*. [Online]. Available: https://www.ncei.noaa.gov/access/billions/

[2] M. Mohler, ''CAL FIRE investigators determine cause of the camp fire,'' California Dept. Forestry Fire Protection, Sacramento, CA, USA, Tech. Rep., 2019.

[3] I. Penn, "PG&E says wildfire victims back settlement in bankruptcy," Tech. Rep., 2020.
[4] (2023). *CAL FIRE Investigators Determine Cause of the Dixie Fire*. [Online]. Available: https://www.fire.ca.gov/media/edwez51p/dixie_fire_release.pdf
[5] (2021). *PG&E Responds to CAL FIRE's Report on 2021 Dixie Fire in Butte, Lassen, Plumas, Shasta, and Tehama Counties*. [Online]. Available: https://s1.q4cdn.com/880135780/files/doc_downloads/2022/06/DIXIE_FINAL_Redacted_PGE-Proposed-Redactions-Statement-49411384.pdf
[6] K. C. Short, *Spatial Wildfire Occurrence Data for the United States, 1992–2020*, document FPA_FOD_20221014, 2020.
[7] S. Jazebi, F. de León, and A. Nelson, "Review of wildfire management techniques—Part I: Causes, prevention, detection, suppression, and data analytics," *IEEE Trans. Power Del.*, vol. 35, no. 1, pp. 430–439, Feb. 2020.
[8] T. Orton. (2011). *Powerline Bushfire Safety Taskforce*. [Online]. Available: https://www.aer.gov.au/system/files/SAPN
[9] S. Bandara, P. Rajeev, and E. Gad, "Power distribution system faults and wildfires: Mechanisms and prevention," *Forests*, vol. 14, no. 6, p. 1146, Jun. 2023.
[10] N. Panossian and T. Elgindy, "Power system wildfire risks and potential solutions: A literature review & proposed metric," U.S. Dept. Energy Office Sci. Tech. Inf., Tech. Rep., 2023.
[11] A. Arab, A. Khodaei, R. Eskandarpour, M. P. Thompson, and Y. Wei, "Three lines of defense for wildfire risk management in electric power grids: A review," *IEEE Access*, vol. 9, pp. 61577–61593, 2021.
[12] W. Jahn, J. L. Urban, and G. Rein, "Powerlines and wildfires: Overview, perspectives, and climate change: Could there be more electricity blackouts in the future?" *IEEE Power Energy Mag.*, vol. 20, no. 1, pp. 16–27, Jan. 2022.
[13] B. Chiu, R. Roy, and T. Tran, "Wildfire resiliency: California case for change," *IEEE Power Energy Mag.*, vol. 20, no. 1, pp. 28–37, Jan. 2022.
[14] E. A. Udren, C. Bolton, D. Dietmeyer, T. Rahman, and S. Flores-Castro, "Managing wildfire risks: Protection system technical developments combined with operational advances to improve public safety," *IEEE Power Energy Mag.*, vol. 20, no. 1, pp. 64–77, Jan. 2022.
[15] D. Sharafi, A. Dowdy, J. Landsberg, P. Bryant, D. Ward, J. Eggleston, and G. Liu, "Wildfires down under: Impacts and mitigation strategies for Australian electricity grids," *IEEE Power Energy Mag.*, vol. 20, no. 1, pp. 52–63, Jan. 2022.
[16] M. Davoudi, B. Efaw, M. Avendaño-Mora, J. L. Lauletta, and G. B. Huffman, "Reclosing of distribution systems for wildfire prevention," *IEEE Trans. Power Del.*, vol. 36, no. 4, pp. 2298–2307, Aug. 2021.
[17] S. Taylor and L. A. Roald, "A framework for risk assessment and optimal line upgrade selection to mitigate wildfire risk," *Electr. Power Syst. Res.*, vol. 213, Dec. 2022, Art. no. 108592.
[18] S. Ghosh and S. Dutta, "A comprehensive forecasting, risk modelling and optimization framework for electric grid hardening and wildfire prevention in the U.S.," *Int. J. Energy Eng.*, vol. 10, no. 3, pp. 80–89, 2020.
[19] R. Bayani, M. Waseem, S. D. Manshadi, and H. Davani, "Quantifying the risk of wildfire ignition by power lines under extreme weather conditions," *IEEE Syst. J.*, vol. 17, no. 1, pp. 1024–1034, Mar. 2023.
[20] N. Rhodes and L. A. Roald, "Co-optimization of power line shutoff and restoration under high wildfire ignition risk," in *Proc. IEEE Belgrade PowerTech*, Jun. 2023, pp. 1–7.
[21] W. Hong, B. Wang, M. Yao, D. Callaway, L. Dale, and C. Huang, "Data-driven power system optimal decision making strategy under wildfire events," Lawrence Livermore Nat. Lab., Livermore, CA, USA, Tech. Rep., 14, 2022.
[22] A. Kody, R. Piansky, and D. K. Molzahn, "Optimizing transmission infrastructure investments to support line de-energization for mitigating wildfire ignition risk," 2022, *arXiv:2203.10176*.
[23] J. M. Johnson, "Quantifying the economic risk of wildfires and power lines in San Diego County," Duke Univ., Durham, NC, USA, Rep., 2014.
[24] B. D. Russell, J. A. Wischkaemper, C. L. Benner, and K. Manivannan, "Preventing certain powerline caused wildfires by early detection and repair of failing devices," in *Proc. IEEE/PES Transmiss. Distrib. Conf. Expo.*, Apr. 2022, pp. 1–5.
[25] J. Ma, J. C. P. Cheng, F. Jiang, V. J. L. Gan, M. Wang, and C. Zhai, "Real-time detection of wildfire risk caused by powerline vegetation faults using advanced machine learning techniques," *Adv. Eng. Informat.*, vol. 44, Apr. 2020, Art. no. 101070.
[26] M. Zhao and M. Barati, "A real-time fault localization in power distribution grid for wildfire detection through deep convolutional neural networks," *IEEE Trans. Ind. Appl.*, vol. 57, no. 4, pp. 4316–4326, Jul. 2021.
[27] S. Kandanaarachchi, N. Anantharama, and M. A. Muñoz, "Early detection of vegetation ignition due to powerline faults," *IEEE Trans. Power Del.*, vol. 36, no. 3, pp. 1324–1334, Jun. 2021.
[28] H. Nazaripouya, "Power grid resilience under wildfire: A review on challenges and solutions," in *Proc. IEEE Power Energy Soc. Gen. Meeting (PESGM)*, Aug. 2020, pp. 1–5.
[29] M. Abdelmalak and M. Benidris, "Enhancing power system operational resilience against wildfires," *IEEE Trans. Ind. Appl.*, vol. 58, no. 2, pp. 1611–1621, Mar. 2022.
[30] D. L. Donaldson, M. S. Alvarez-Alvarado, and D. Jayaweera, "Power system resiliency during wildfires under increasing penetration of electric vehicles," in *Proc. Int. Conf. Probabilistic Methods Appl. Power Syst. (PMAPS)*, Aug. 2020, pp. 1–6.
[31] R. Bayani and S. D. Manshadi, "Resilient expansion planning of electricity grid under prolonged wildfire risk," *IEEE Trans. Smart Grid*, vol. 13, no. 1, pp. 1–10, Jan. 2023.
[32] W. Yang, S. N. Sparrow, M. Ashtine, D. C. H. Wallom, and T. Morstyn, "Resilient by design: Preventing wildfires and blackouts with microgrids," *Appl. Energy*, vol. 313, May 2022, Art. no. 118793.
[33] R. Moreno, D. N. Trakas, M. Jamieson, M. Panteli, P. Mancarella, G. Strbac, C. Marnay, and N. Hatziargyriou, "Microgrids against wildfires: Distributed energy resources enhance system resilience," *IEEE Power Energy Mag.*, vol. 20, no. 1, pp. 78–89, Jan. 2022.
[34] Q. A. Saeed and H. Nazaripouya, "Impact of wildfires on power systems," in *Proc. IEEE Int. Conf. Environ. Electr. Eng. IEEE Ind. Commercial Power Syst. Eur.*, Jun. 2022, pp. 1–5.
[35] M. Choobineh, B. Ansari, and S. Mohagheghi, "Vulnerability assessment of the power grid against progressing wildfires," *Fire Saf. J.*, vol. 73, pp. 20–28, Apr. 2015.
[36] A. Malik, M. R. Rao, N. Puppala, P. Koouri, V. A. K. Thota, Q. Liu, S. Chiao, and J. Gao, "Data-driven wildfire risk prediction in northern California," *Atmosphere*, vol. 12, no. 1, p. 109, Jan. 2021.
[37] J. W. Mitchell, "Power line failures and catastrophic wildfires under extreme weather conditions," *Eng. Failure Anal.*, vol. 35, pp. 726–735, Dec. 2013.
[38] D. A. Dawe, M. Parisien, Y. Boulanger, J. Boucher, A. Beauchemin, and D. Arseneault, "Short and long-term wildfire threat when adapting infrastructure for wildlife conservation in the boreal forest," *Ecol. Appl.*, vol. 32, no. 6, pp. e2606, Sep. 2022.
[39] R. Zhang, R. Zhong, Y. Pang, B. Yang, and H. Shu, "Risk assessment of high voltage power lines crossing forest areas—A case study of wildfires," *ISPRS Ann. Photogramm., Remote Sens. Spatial Inf. Sci.*, vol. 3, pp. 199–206, Oct. 2022.
[40] M. A. Finney, "FARSITE: Fire area simulator-model development and evaluation," U.S. Dept. Agricult., Washington, DC, USA, Rep., 1988.
[41] *Illinois Center for a Smarter Electric Grid (ICSEG)*. Accessed: Apr. 1, 2024. [Online]. Available: https://icseg.iti.illinois.edu/ieee-30-bus-system
[42] G. D. Papadopoulos and F.-N. Pavlidou, "A comparative review on wildfire simulators," *IEEE Syst. J.*, vol. 5, no. 2, pp. 233–243, Jun. 2011.
[43] M. P. Nicolau et al., "Large forest fire risk assessment and fuel management: Operational tools and integrated approach," in *Fire Efficient, Operational Tools for Improving Efficiency in Wildfire Risk Reduction in EU Landscapes*. European Union, Sep. 2014.
[44] P. N. Yasasvi, S. Chandra, A. Mohapatra, and S. C. Srivastava, "An exact SOCP formulation for AC optimal power flow," in *Proc. 20th Nat. Power Syst. Conf. (NPSC)*, Dec. 2018, pp. 1–6.
[45] M. G. Rollins, "LANDFIRE: A nationally consistent vegetation, wildland fire, and fuel assessment," *Int. J. Wildland Fire*, vol. 18, no. 3, p. 235, 2009.
[46] *National Renewable Energy Laboratory (NREL)*. Accessed: Apr. 1, 2024. [Online]. Available: https://nsrdb.nrel.gov
[47] R. M. S. Pinto, A. Benali, A. C. L. Sá, P. M. Fernandes, P. M. M. Soares, R. M. Cardoso, R. M. Trigo, and J. M. C. Pereira, "Probabilistic fire spread forecast as a management tool in an operational setting," *SpringerPlus*, vol. 5, no. 1, pp. 1–23, Dec. 2016.

BEHROUZ SOHRABI (Member, IEEE) received the Master of Science degree in computer engineering from the University of Denver, with a focus on data science applications in power systems and the energy industry. His thesis was ''Data-driven Solutions for Transmission and Distribution Networks in Modern Power Grids,'' reflects a keen interest in the integration of computational techniques with energy systems. He is dedicated to leveraging advanced software-based technologies in solving complex problems in the energy sector. His research interests include center on exploring innovative, data-driven strategies to enhance the efficiency, and resilience of modern power grids.

ALI ARABNYA (ALI ARAB) (Senior Member, IEEE) received the Ph.D. degree in industrial engineering from the University of Houston, Houston, TX, USA, in 2015. He is currently the Director of the Infrastructure Finance and Climate Risk, Quanta Technology, Raleigh, NC, USA, and a Research Professor of electrical and computer engineering with the University of Denver, Denver, CO, USA. Previously, he was a Consultant Climate Economist with the World Bank Group, Washington, DC, USA. Prior to that, he was a Data and Analytics Manager with Protiviti, New York, NY, USA. He is the co-author of one book and more than 30 technical papers in flagship journals and conference proceedings. He served as the Guest Editor-in-Chief for the Special Issue on Climate Change Mitigation and Adaptation with *International Journal of Electrical Power and Energy Systems*. His research interests include smart grid resilience, artificial intelligence, decarbonization, and climate finance.

MATTHEW P. THOMPSON received the B.S. degree in systems engineering from the University of Virginia, the M.S. degree in industrial engineering and operations research from the University of California, Berkeley, and the M.S. and Ph.D. degrees in forest management from Oregon State University. He is the Director of Applied Fire Science at Pyrologix, a subsidiary of Vibrant Planet. Prior to joining Pyrologix, he spent 14 years in the Human Dimensions Program at the USDA Forest Service Rocky Mountain Research Station. His research interests focus primarily on risk, systems, strategy, and decision analysis. He received a professional certificate in strategic decision and risk management from Stanford University and he was a Senior Executive Fellow at the Harvard Kennedy School.

AMIN KHODAEI (Senior Member, IEEE) is currently a Professor and the Past Chair of the Electrical and Computer Engineering Department, University of Denver. He has authored more than 200 peer-reviewed technical articles and has advised more than 40 graduate students and postdoctoral associates. He is the co-author of an IEEE/Wiley-published book titled *The Economics of Microgrids*. His research interests include climate crisis, the grid of the future, and advanced technologies to modernize the grid, including artificial intelligence and quantum computing. As an Active Member of the IEEE, he has served as the Technical Chair of the 2016 and 2018 IEEE PES T&D Conferences and the Technical Chair of the 2022 IEEE PES General Meeting.